Dynamic ADMM for Real-Time Optimal Power Flow

Preprint

Yijian Zhang and Mingyi Hong
Iowa State University

Emiliano Dall'Anese
National Renewable Energy Laboratory

Presented at the 2017 5th IEEE Global Conference on Signal and Information Processing (GlobalSIP)
Montreal, Canada
November 14-16, 2017

© 2017 IEEE. Personal use of this material is permitted. Permission from IEEE must be obtained for all other uses, in any current or future media, including reprinting/republishing this material for advertising or promotional purposes, creating new collective works, for resale or redistribution to servers or lists, or reuse of any copyrighted component of this work in other works.

NREL is a national laboratory of the U.S. Department of Energy
Office of Energy Efficiency & Renewable Energy
Operated by the Alliance for Sustainable Energy, LLC

This report is available at no cost from the National Renewable Energy Laboratory (NREL) at www.nrel.gov/publications.

Conference Paper
NREL/CP-5D00-68625
February 2018

Contract No. DE-AC36-08GO28308

NOTICE

The submitted manuscript has been offered by an employee of the Alliance for Sustainable Energy, LLC (Alliance), a contractor of the US Government under Contract No. DE-AC36-08GO28308. Accordingly, the US Government and Alliance retain a nonexclusive royalty-free license to publish or reproduce the published form of this contribution, or allow others to do so, for US Government purposes.

This report was prepared as an account of work sponsored by an agency of the United States government. Neither the United States government nor any agency thereof, nor any of their employees, makes any warranty, express or implied, or assumes any legal liability or responsibility for the accuracy, completeness, or usefulness of any information, apparatus, product, or process disclosed, or represents that its use would not infringe privately owned rights. Reference herein to any specific commercial product, process, or service by trade name, trademark, manufacturer, or otherwise does not necessarily constitute or imply its endorsement, recommendation, or favoring by the United States government or any agency thereof. The views and opinions of authors expressed herein do not necessarily state or reflect those of the United States government or any agency thereof.

This report is available at no cost from the National Renewable Energy Laboratory (NREL) at www.nrel.gov/publications.

Available electronically at SciTech Connect http:/www.osti.gov/scitech

Available for a processing fee to U.S. Department of Energy and its contractors, in paper, from:

U.S. Department of Energy
Office of Scientific and Technical Information
P.O. Box 62
Oak Ridge, TN 37831-0062
OSTI http://www.osti.gov
Phone: 865.576.8401
Fax: 865.576.5728
Email: reports@osti.gov

Available for sale to the public, in paper, from:

U.S. Department of Commerce
National Technical Information Service
5301 Shawnee Road
Alexandria, VA 22312
NTIS http://www.ntis.gov
Phone: 800.553.6847 or 703.605.6000
Fax: 703.605.6900
Email: orders@ntis.gov

Cover Photos by Dennis Schroeder: (left to right) NREL 26173, NREL 18302, NREL 19758, NREL 29642, NREL 19795.

NREL prints on paper that contains recycled content.

DYNAMIC ADMM FOR REAL-TIME OPTIMAL POWER FLOW

Yijian Zhang[1], *Emiliano Dall'Anese*[2], *and Mingyi Hong*[1]

[1]Industrial and Manufacturing Systems Engineering, Iowa State University, Ames, IA 50011, USA
[2]National Renewable Energy Laboratory, Golden, CO 80401, USA

ABSTRACT

This paper considers distribution networks featuring distributed energy resources (DERs), and develops a dynamic optimization method to maximize given operational objectives in real time while adhering to relevant network constraints. The design of the dynamic algorithm is based on suitable linearization of the AC power flow equations, and it leverages the so-called alternating direction method of multipliers (ADMM). The steps of the ADMM, however, are suitably modified to accommodate appropriate measurements from the distribution network and the DERs. With the aid of these measurements, the resultant algorithm can enforce given operational constraints in spite of inaccuracies in the representation of the AC power flows, and it avoids ubiquitous metering to gather the state of noncontrollable resources. Optimality and convergence of the proposed algorithm are established in terms of tracking of the solution of a convex surrogate of the AC optimal power flow problem.

1. INTRODUCTION

This paper focuses on *real-time* management of distributed energy resources (DERs) in distribution systems. Notwithstanding the variability of ambient conditions and noncontrollable energy assets [1], real-time optimization methods can adjust the power setpoints of the DERs on a second or subsecond level to maximize the performance objectives and systematically enforce operational constraints. Challenges in this context are related to computational and logistic considerations, which render infeasible solution of optimization problems such as the AC optimal power flow (OPF) on a second or subsecond timescale [2].

In lieu of a batch solution approach, dynamic (sometimes also referred to as "online") algorithms for real-time optimization of power systems are proposed in [3–6], where measurements of the output powers of given devices were used as a proxy for optimization variables in primal-dual-type methods. A similar approach was explored in [7], where a centralized controller was developed based on projected-gradient methods, and in [8], where the alternating direction method of multipliers (ADMM) [9, 10] was utilized for the design of a distributed online algorithm. Recently, a projected-gradient method on the (static) power flow manifold was proposed in [11],a projected-gradient method on the power flow manifold was proposed in [11,12], while a real-time algorithm for relaxed AC OPF problems based on quasi-Newton methods was developed in [13]. A distributed dynamic algorithm based on primal-dual methods and double-smoothing techniques [14] was developed in [15]; voltage measurements were embedded in the primal and dual steps to enforce voltage constraints in spite of inaccuracies in the representation of the AC power flows. Convergence was established in terms of tracking of solutions of a time-varying linearized AC OPF.

In this paper, we start from the formulation of a *time-varying* linearized AC OPF problem capturing a variety of DER-oriented objectives as well as voltage constraints. We also consider constraints on the active power at the point of coupling, in line with the emerging vision of feeders providing ancillary services to the grid [16–18]. We then design a dynamic algorithm by leveraging the ADMM. The steps of the ADMM, however, are suitably modified to accommodate appropriate measurements from the distribution network and the DERs. With the aid of these measurements, the resultant algorithm can enforce operational constraints in spite of inaccuracies in the representation of the AC power flows, and it avoids pervasive metering to collect measurements of the state of non-controllable assets. Convergence of the propose algorithm are established in terms of tracking of the solution of a linearized AC OPF problem.

Overall, we extend our previous work [8] by i) incorporating voltage and power flow measurements into the ADMM iterations, and ii) providing convergence results in terms of tracking of the solution of a time-varying optimization problem. Relative to [15], the proposed approach enables one to establish convergence without assuming Lipschitz continuity of the gradient of the objective function.

2. PROBLEM FORMULATION

Consider a (portion of a) distribution network with $N+1$ nodes collected in the set $\mathcal{N} \cup \{0\}$, where 0 denotes the point of coupling with the rest of the grid. Assume that temporal domain is discretized as $t = k\tau$, $k \in \mathbb{N}$ and $\tau > 0$. At time $k\tau$, define the vector $\mathbf{i}^k := [I_1^k, \ldots, I_N^k]^\top \in \mathbb{C}^N$, where I_n^k denotes the phasor of the current injected at node n. Let $\mathbf{v}^k := [V_1^k, \ldots, V_N^k]^\top \in \mathbb{C}^N$, where $V_i^k = |V_i^k| \angle \theta_i \in \mathbb{C}$ denotes the voltage phasor at node i, where $V_0^k e^{j\theta_0}$ is the slack-bus voltage with V_0^k denoting the voltage magnitude. Let $P_i^k + jQ_i^k$ denote the setpoints of DER $i \in \mathcal{N}_D$, and define $\mathbf{u}_i^k := [P_i^k, Q_i^k]^\top$ for brevity. Similarly, let $P_{l,i}^k + jQ_{l,i}^k$ denote the (non-controllable) net power demanded at node $i \in \mathcal{N}$ and $\mathbf{d}_i^k := [P_{l,i}^k, Q_{l,i}^k]^\top$. Based on Kirchhoff's Current Law and Ohm's Law we can establish the following linear relationship:

$$\begin{bmatrix} I_0^k \\ \mathbf{i}^k \end{bmatrix} = \begin{bmatrix} y_{00}^k & (\bar{\mathbf{y}}^k)^\top \\ \bar{\mathbf{y}}^k & \mathbf{Y}^k \end{bmatrix} \begin{bmatrix} V_0^k e^{j\theta_0} \\ \mathbf{v}^k \end{bmatrix}, \tag{1}$$

where submatrices $\mathbf{Y}^k \in \mathbb{C}^{N \times N}$, $\bar{\mathbf{y}}^k \in \mathbb{C}^{N \times 1}$, $y_{00}^k \in \mathbb{C}$ are formed based on the system topology and π-equivalent model of the distribution lines (see e.g. [19]).

At time $k\tau$ a prototypical AC OPF formulation is given as follows:

This work was supported by the Laboratory Directed Research and Development Program at the National Renewable Energy Laboratory. The work of E. Dall'Anese was also supported by the Advanced Research Projects Agency-Energy (ARPA-E) under the Network Optimized Distributed Energy Systems (NODES) program.

This report is available at no cost from the National Renewable Energy Laboratory (NREL) at www.nrel.gov/publications.

$$\min_{\{\mathbf{v},\mathbf{i},P_i,Q_i\}} \sum_{i\in\mathcal{N}_D} f_i^k(P_i,Q_i) \tag{2a}$$

$$\text{s.t.} \quad \mathbf{i} = \mathbf{Y}^k \mathbf{v}, \tag{2b}$$

$$V_i I_i^* = P_i - P_{l,i}^k + j(Q_i - Q_{l,i}^k), \forall i \in \mathcal{N}_D, \tag{2c}$$

$$V_i I_i^* = -P_{l,i}^k - jQ_{l,i}^k, \forall i \in \mathcal{N}_O, \tag{2d}$$

$$V^{\min} \le |V_n| \le V^{\max}, \forall n \in \mathcal{M}, \tag{2e}$$

$$(P_i, Q_i) \in \mathcal{Y}_i^k, \forall i \in \mathcal{N}_D, \tag{2f}$$

where $\mathcal{N}_D$ and $\mathcal{N}_O$ denote a subset of nodes with or without DER inverters, respectively; $\mathcal{M}$ denotes a subset of nodes where measurements of the voltage magnitudes can be obtained, $\mathcal{Y}_i^k$ is a convex compact set modeling the operational constraints of the DER i; and, $V^{\min}$ and $V^{\max}$ denote the minimum and maximum voltage service limits. Finally, the time-varying function $f_i^k(P_i, Q_i)$ is assumed to be strongly convex and it specifies customer-oriented performance objectives (e.g. cost or reward for ancillary service provisioning). Problem (2) will be modified in Section 3.2 to account for additional operational objectives.

Problem (2) is a *time-varying nonconvex optimization problem*. Solving (P1)$^{(k)}$ in batch fashion at each time k is impractical because of the following two main challenges:
c1) For real-time implementations (e.g., when τ is on the order of a second or subsecond), it might be unfeasible to solve (2) to convergence.
c2) Solving (2) requires collecting measurements of the noncontrollable loads at all locations in real time.

To address these challenges, we first leverage appropriate linearizations of the AC power-flow equations [20–22] to formulate a convex surrogate of (2). We will then design a *feedback-based dynamic ADMM method* that produces provably-optimal setpoints for DERs, while coping with approximation errors and avoiding ubiquitous monitoring.

3. ADMM-BASED REAL-TIME OPF

We leverage the following approximate linear relationship between voltage magnitudes and net injected power:

$$|V_n^k| \approx \sum_{i\in\mathcal{N}_D} [r_{n,i}^k(P_i - P_{l,i}^k) + b_{n,i}^k(Q_i - Q_{l,i}^k)] + \bar{a}_n^k \tag{3a}$$

$$\bar{a}_n^k := a_n^k - \sum_{i\in\mathcal{N}} (r_{n,i}^k P_{l,i}^k + b_{n,i}^k Q_{l,i}^k), \tag{3b}$$

where the model parameters $\mathbf{R} = [r_{n,i}] \in \mathbb{R}^{N\times N}, \mathbf{B} = [b_{n,i}] \in \mathbb{R}^{N\times N}$, and $\mathbf{a}^k = [a_n^k] \in \mathbb{R}^N$ can be derived as shown in e.g., [20–22]. Using (3), a convex surrogate of (2) can be formulated as follows:

$$\min_{\mathbf{p},\mathbf{q}} \quad \sum_{i\in\mathcal{N}_D} f_i^k(\mathbf{u}_i) \tag{4a}$$

$$\text{s.t.} \quad g_n^k(\{\mathbf{u}_i\}_{i\in\mathcal{N}_D}) \le 0, \forall n \in \mathcal{M}, \tag{4b}$$

$$\bar{g}_n^k(\{\mathbf{u}_i\}_{i\in\mathcal{N}_D}) \le 0, \forall n \in \mathcal{M}, \tag{4c}$$

$$\mathbf{u}_i \in \mathcal{Y}_i^k, \tag{4d}$$

where the inequality constraints (4b)–(4c) are given by:

$$g_n^k(\{\mathbf{u}_i\}_{i\in\mathcal{N}_D}) = V^{\min} - \bar{a}_n^k - \sum_{i\in\mathcal{N}_D} (r_{n,i}^k P_i + b_{n,i}^k Q_i) \le 0,$$

$$\bar{g}_n^k(\{\mathbf{u}_i\}_{i\in\mathcal{N}_D}) = \bar{a}_n^k + \sum_{i\in\mathcal{N}_D} (r_{n,i}^k P_i + b_{n,i}^k Q_i) - V^{\max} \le 0.$$

To facilitate the development of a dynamic ADMM-based algorithm, it is convenient to find a reformulation (or relaxation) of (4) in the following form

$$\min_{x\in\mathcal{X}, y\in\mathcal{Y}} \quad h(x) + g(y) \qquad \text{s.t.} \quad Ax + By = 0, \tag{5}$$

where $h(\cdot)$ and $g(\cdot)$ are strongly convex functions; the gradient ∇f is Lipschitz continuous; and, the matrix A is full row rank. To this end, one can utilize the following steps:
i) Add slack variables $z_n \ge 0, y_n \ge 0$ for (4b) and (4c);
ii) Transfer the nonnegative constraints $z_n \ge 0$ and $y_n \ge 0$ to the objective using a max function;
iii) Use a smooth function $h(\cdot)$ to approximate the max function;
iv) Add a small term strongly convex w.r.t. $\mathbf{z}, \mathbf{y}$.
Using steps i)-iv), a relaxed version of (4) can be stated as follows:

$$\min_{\mathbf{p},\mathbf{q},\mathbf{z},\mathbf{y}} \epsilon(\|\mathbf{z}\|^2 + \|\mathbf{y}\|^2) + \gamma(h(\mathbf{z}) + h(\mathbf{y})) + \sum_{i\in\mathcal{N}_D} f_i^k(\mathbf{u}_i) \tag{6a}$$

$$\text{s.t.}\ g_n^k(\{\mathbf{u}_i\}_{i\in\mathcal{N}_D}) + z_n = 0, \forall n \in \mathcal{M}, \tag{6b}$$

$$\bar{g}_n^k(\{\mathbf{u}_i\}_{i\in\mathcal{N}_D}) + y_n = 0, \forall n \in \mathcal{M}, \tag{6c}$$

$$\mathbf{u}_i \in \mathcal{Y}_i^k, \forall i \in \mathcal{N}_D$$

where $\epsilon > 0$ is set to be a very small constant, $\gamma > 0$ is set to be a large constant so as to enforce nonnegativity of the slack variables, and the smooth approximation $h(\mathbf{x}) = (\dots; h(x_n); \dots)$ can take the following form ($a > 0$ is a given constant that close to 0)

$$h(x_n) = \begin{cases} -x_n, & x_n \in (-\infty, -a], \\ \frac{-1}{4a}(x_n - a)^2, & x_n \in [-a, a], \\ 0, & x_n \in [a, +\infty)\,. \end{cases}$$

Problem (6) is a *time-varying convex optimization problem*. In the following section, we will develop a *feedback-based dynamic ADMM method* to track the optimal solution of (6) over time. With the aid of appropriate measurements, voltage constraints will be enforced even if we rely on an approximate power flow model.

3.1. Algorithm

Consider the following augmented Lagrangian function

$$\begin{aligned}\mathcal{L}(\mathbf{u},\mathbf{z},\mathbf{y};\lambda,\mu) = {} & \epsilon \sum_{n\in\mathcal{M}} (\|z_n\|^2 + \|y_n\|^2) \\ & + \gamma \sum_{n\in\mathcal{M}} (h(z_n) + h(y_n)) + \sum_{i\in\mathcal{N}_D} f_i^k(\mathbf{u}_i) \\ & + \frac{\rho}{2} \sum_{n\in\mathcal{M}} (g_n^k(\{\mathbf{u}_i\}_{i\in\mathcal{N}_D}) + z_n + \frac{\lambda_n}{\rho})^2 \\ & + \frac{\rho}{2} \sum_{n\in\mathcal{M}} (\bar{g}_n^k(\{\mathbf{u}_i\}_{i\in\mathcal{N}_D}) + y_n + \frac{\mu_n}{\rho})^2,\end{aligned}$$

where λ_n, μ_n are the Lagrangian multipliers associated with (6b)–(6c) and $\rho > 0$ is a given constants. Assume, for now, that functions $f_i^k(\mathbf{u}_i)$, $i \in \mathcal{N}_D$ are differentiable. Relative to standard ADMM implementations [9, 10], the proposed approach involves the following three modifications in order to enable a distributed implementation, avoid pervasive metering to collect measurements of $\{P_{l,i}^k, Q_{l,i}^k\}$ at each time k, and cope with approximation errors:

This report is available at no cost from the National Renewable Energy Laboratory (NREL) at www.nrel.gov/publications.

(m1) Let $|\hat{V}_n^k|$ denote a measurement of the voltage magnitude $|V_n^k|$. Then, in the steps of the ADMM, replace g_n^k and $\bar{g}_n^k$ with the following measurement:

$$g_n^k(\{\mathbf{u}_i\}_{i\in\mathcal{N}_D}) \leftrightarrow V^{\min} - |\hat{V}_n^k|,$$
$$\bar{g}_n^k(\{\mathbf{u}_i\}_{i\in\mathcal{N}_D}) \leftrightarrow |\hat{V}_n^k| - V^{\max}.$$

(m2) Since the optimization variables pertaining to different DERs are coupled in the augmented Lagrangian, it is not possible to distributed the update $\{P_i^k, Q_i^k\}$ across DERs. This, we propose to update $\{P_i^k, Q_i^k\}$ based on the following projected-gradient step:

$$\begin{pmatrix} P_i^k \\ Q_i^k \end{pmatrix} = \mathrm{proj}_{\mathcal{Y}_i^k}\begin{pmatrix} P_i^{k-1} - \alpha \frac{\partial \mathcal{L}}{\partial P_i}|_{P_i^{k-1}, Q_i^{k-1}} \\ Q_i^{k-1} - \alpha \frac{\partial \mathcal{L}}{\partial Q_i}|_{P_i^{k-1}, Q_i^{k-1}} \end{pmatrix} \tag{7}$$

where $\mathrm{proj}_{\mathcal{Y}}(x) := \arg\min_{y\in\mathcal{Y}} \|y - x\|_2$ denotes projection onto the convex set $\mathcal{Y}$ and:

$$\frac{\partial \mathcal{L}}{\partial P_i} = \frac{\partial f_i^{k-1}}{\partial P_i} + \rho \sum_{n\in\mathcal{M}} (-r_{n,i}^{k-1})(V^{\min} - |\hat{V}_n^{k-1}| + z_n + \frac{\lambda_n}{\rho})$$
$$+ \rho \sum_{n\in\mathcal{M}} r_{n,i}^{k-1}(|\hat{V}_n^{k-1}| - V^{\max} + y_n + \frac{\mu_n}{\rho}) \tag{8}$$
$$\frac{\partial \mathcal{L}}{\partial Q_i} = \frac{\partial f_i^{k-1}}{\partial Q_i} + \rho \sum_{n\in\mathcal{M}} (-b_{n,i}^{k-1})(V^{\min} - |\hat{V}_n^{k-1}| + z_n + \frac{\lambda_n}{\rho})$$
$$+ \rho \sum_{n\in\mathcal{M}} b_{n,i}^{k-1}(|\hat{V}_n^{k-1}| - V^{\max} + y_n + \frac{\mu_n}{\rho})\,. \tag{9}$$

Notice that, based on (m1), the update (7) includes voltage measurements instead of functions g_n^k and $\bar{g}_n^k$.

(m3) Variables $\mathbf{z}, \mathbf{y}$ are updated by setting the gradients of the augmented Lagrangian with respect to $\mathbf{z}^k, \mathbf{y}^k$ to 0:

$$\frac{\partial \mathcal{L}}{\partial \mathbf{z}^k} = 2\epsilon \mathbf{z}^k + \gamma \nabla h(\mathbf{z}^k) + \rho(V^{\min}\mathbf{1} - |\hat{\mathbf{v}}^k| + \mathbf{z}^k + \frac{\lambda^{k-1}}{\rho}) = \mathbf{0}$$
$$\frac{\partial \mathcal{L}}{\partial \mathbf{y}^k} = 2\epsilon \mathbf{y}^k + \gamma \nabla h(\mathbf{y}^k) + \rho(|\hat{\mathbf{v}}^k| - V^{\max}\mathbf{1} + \mathbf{y}^k + \frac{\mu^{k-1}}{\rho}) = \mathbf{0}\,.$$

Based on the specific choice of the parameters in $h(\cdot)$, a closed-form solution can be derived.

With these modifications in place, the resultant algorithm is summarized below.

Algorithm 1 Dynamic ADMM with feedback

At each time $k = 1, 2, \ldots$:

[S1] For each $i \in \mathcal{N}_D$, update P_i^k, Q_i^k via (7) based on the most up to date measurements.

[S2] Collect voltage measurements $|\hat{V}_n^k|, n \in \mathcal{M}$.

[S3] For each $n \in \mathcal{M}$, update auxiliary variables z_n^k, y_n^k.

[S4] For each $n \in \mathcal{M}$, update dual variables λ_n^k, μ_n^k as

$$\lambda_n^k = \lambda_n^{k-1} + \rho(V^{\min} - |\hat{V}_n^k| + z_n^k), n \in \mathcal{M} \tag{10a}$$
$$\mu_n^k = \mu_n^{k-1} + \rho(|\hat{V}_n^k| - V^{\max} + y_n^k), n \in \mathcal{M}. \tag{10b}$$

Notice that the Algorithm 1 does not require one to collect information regarding the noncontrollable loads $\{P_{l,i}^k, Q_{l,i}^k, i \in \mathcal{N}\}$ at each time k.

3.2. Adding operational constraints

As an illustrative example to show how to include additional operational constraints, consider the case where setpoints for the real power withdrawn from the point of coupling with the main grid are specified and must be tracked over time [16, 17]. The active power at the point of coupling can be expressed as $P_0^k = \Re\{|V_0^k|^2(y_{01}^* + y_0^*) - V_0^k(y_{01}^*(V_1^k)^*)\}$ and it is nonlinearly related to the net powers injected in the rest of the network. However, we can utilize the linear approximation of the AC power-flow equations of [22], e.g., $P_0^k(\mathbf{u}) \approx \sum_{i\in\mathcal{N}_D}(m_i^k P_i^k + n_i^k Q_i^k) + c^k$ (see [22] for a detailed derivation of m_i^k, n_i^k, and c^k) to synthesize the ADMM-based algorithm.

Denote as $P_{0,\text{set}}^k$ the setpoint for P_0 at time k, and consider the following constraints:

$$\bar{h}^k(P_0(\mathbf{u}) - P_{0,\text{set}}) \le E^k, \quad \bar{h}^k(P_{0,\text{set}} - P_0(\mathbf{u})) \le E^k, \tag{11}$$

where $\bar{h}^k = 1$ if the network is requested to follow the setpoint and $\bar{h}^{t_k} = 0$ otherwise, while $E^k > 0$ is a given tracking error. Consider then adding slack variables τ and κ, and consider the following problem formulation:

$$\min_{\mathbf{p},\mathbf{q},\mathbf{z},\mathbf{y}} \epsilon(\|\mathbf{z}\|^2 + \|\mathbf{y}\|^2 + \tau^2 + \kappa^2) + \gamma(h(\mathbf{z}) + h(\mathbf{y}) + h(\tau) + h(\kappa))$$
$$+ \sum_{i\in\mathcal{N}_D} f_i^k(\mathbf{u}_i) \tag{12a}$$
$$\text{s.t. } g_n^k(\{\mathbf{u}_i\}_{i\in\mathcal{N}_D}) + z_n = 0, \forall n \in \mathcal{M}, \tag{12b}$$
$$\bar{g}_n^k(\{\mathbf{u}_i\}_{i\in\mathcal{N}_D}) + y_n = 0, \forall n \in \mathcal{M}, \tag{12c}$$
$$\bar{h}^k(P_0^k(\mathbf{u}) - P_{0,set}^k) + \tau = E^k, \tag{12d}$$
$$\bar{h}^{t_k}(P_{0,set}^k - P_0^k(\mathbf{u})) + \kappa = E^k, \tag{12e}$$
$$\mathbf{u}_i \in \mathcal{Y}_i^k. \tag{12f}$$

Based on (12), a dynamic ADMM-based algorithm can then be derived by following the procedure outlined in Section 3.1. In par with (m1), in the resultant algorithm the algorithmic quantity $P_0^k(\mathbf{u}^k)$ is replaced with a measurement $\hat{P}_0^k$ of the power at the point of coupling at time k. The algorithm is not presented for space limitations.

4. CONVERGENCE ANALYSIS

In this section, we provide analytical results for the convergence and tracking capabilities of the dynamic algorithm. We focus our analysis on the problem (12).

Since (12) is a time-varying problem, it is appropriate to introduce the bounds $\|\mathbf{u}^{*,k+1} - \mathbf{u}^{*,k}\| \le \sigma_u$ and $\|\boldsymbol{\eta}^{*,k+1} - \boldsymbol{\eta}^{*,k}\| \le \sigma_\eta$, where $\boldsymbol{\eta} = (\mathbf{z}, \mathbf{y}, \tau, \kappa)$, which capture the temporal variability of the optimal solution of (12) (σ_u, σ_η are some constants). Further, we indroduce the following assumptions to capture the temporal variability of the dual variables and to bound the measurement and approximation errors.

Assumption 1. *There exists a constant $0 \le e \le +\infty$ so that the measurement and approximation errors can be bounded for every n and k as:*

$$\left||\hat{V}_n^k| - g_n^k(\mathbf{u}^k)\right| \le e, \ \left||\hat{V}_n^k| - \bar{g}_n^k(\mathbf{u}^k)\right| \le e, \tag{13}$$
$$\left|\hat{P}_0^k - \sum_{i\in\mathcal{N}_D}(m_i^k P_i^k + n_i^k Q_i^k) + c^k\right| \le e. \tag{14}$$

This report is available at no cost from the National Renewable Energy Laboratory (NREL) at www.nrel.gov/publications.

Assumption 2. *There exists a constant $\sigma_\psi \geq 0$ such that*

$$\|\boldsymbol{\psi}^{*,k+1} - \boldsymbol{\psi}^{*,k}\| \leq \sigma_\psi, \tag{15}$$

where $\boldsymbol{\psi} = (\lambda, \mu, \nu_1, \nu_2)$, and ν_1, ν_2 are the dual variables associated with (12d)–(12e)*.*

In the spirit of [14], future efforts will establish conditions on the variability of the primal problem that imply (15). Based on these assumptions, the following result holds (the proof is omitted due to space limitations).

Theorem 1. *Define $\mathbf{w} := (\boldsymbol{\eta}; \mathbf{u}; \boldsymbol{\psi})$ and let $\{\mathbf{w}^k\}$ be the sequence generated by Algorithm 1. Further, let $\mathbf{w}^{*,k}$ be an optimal solution of* (12) *at time k. Then,*

$$\lim_{k\to\infty} \sup \|\mathbf{w}^k - \mathbf{w}^{*,k}\|_2 = \frac{\alpha(e)}{1-r} + \frac{r\beta(\sigma)}{1-r}, \tag{16}$$

where $0 < r < 1$, $\alpha(e) = \frac{\rho e}{\epsilon} + 4\rho e + \alpha\rho e \sum_{i,n}(r_{n,i} + b_{n,i})$ and $\beta(\sigma) = \sigma_u + \sigma_\eta + \sigma_\psi$.

The result (16) bounds the maximum discrepancy between the setpoints produced by Algorithm 1 and the time-varying optimizer of (12) at any time k.

One of the advantages of ADMM compared to the double-smoothing-based scheme in [15] (see also [14]) is that the convergence claims are still valid when the functions $f_i^k(P_i, Q_i), i \in \mathcal{N}_D$, are *nonsmooth*. In this case, step (7) is replaced by a proximal gradient step. For example, is function $f_i(P_i, Q_i)$ takes the form $f_i(P_i, Q_i) = c_q Q_i^2 + \bar{c}_q |Q_i| + c_p P_i^2$, the proximal-gradient step boils down to:

$$\begin{pmatrix} P_i^{k+1} \\ Q_i^{k+1} \end{pmatrix} = \mathrm{proj}_{\mathcal{Y}_i} \begin{pmatrix} P_i^k - t_k \frac{\partial \mathcal{L}}{\partial P_i}|_{P_i^k, Q_i^k} \\ \mathrm{soft}_{\bar{c}_q}(Q_i^k - l_k \frac{\partial \mathcal{L}}{\partial Q_i}|_{P_i^k, Q_i^k}) \end{pmatrix},$$

where $\mathrm{soft}_x(y) = \mathrm{sign}(y) \cdot \max(|y| - x, 0)$ is the soft-threshold operator.

5. NUMERICAL EXPERIMENTS

As an illustrative example, we test the proposed algorithm on the test system considered in [15]. Particularly, the test cases utilizes a modified IEEE 37-node test feeder, where the network is obtained by considering a single phase equivalent, and by replacing the loads on phase "c" specified in the original dataset with real load data measured from feeders in a neighborhood called Anatolia in California during a week in August 2012 [23]. It is assumed that aggregations of photovoltaic (PV) systems are located at nodes 4, 7, 10, 13, 17, 20, 22, 23, 26, 28, 29, 30, 31, 32, 33, 34, 35, and 36 (see [15] for the numbering). The rating of these inverters are 300 kVA for $i = 3$, 350 kVA for $i = 15, 16$, and 200 kVA for the remaining ones.

The optimization objective is chosen to be $f_i(P_i, Q_i) = c_p(P_{\text{av},i} - P_i)^2 + c_q(Q_i)^2 + \bar{c}_q|Q_i|$, where $P_{\text{av},i}$ is the maximum real power available from the PV system i, and $c_p = 3, c_q = 1, \bar{c}_q = 0.1$. The voltage limits are set to be $V^{\min} = 0.95$pu, $V^{\max} = 1.05$pu. The generation profiles are simulated based on real solar irradiance data and have a granularity of 1 second.

We specify a given trajectory for the power at the common coupling, which is color-coded in red in Fig. 1 (negative power indicates reverse power flows). It can be seen that our algorithm is able to regulate P_0^k close to $P_{0,\text{set}}^k$ in real time. Figure 2 illustrates the voltage profiles for selected nodes. It can be seen that voltage regulation is enforced and a flat voltage profile is obtained. A comparison with double smoothing algorithm [15] is presented in Figure 3. The proposed strategy has potentially better voltage regulation ability, especially for extreme cases e.g. the two spikes from 10:00 to 12:00.

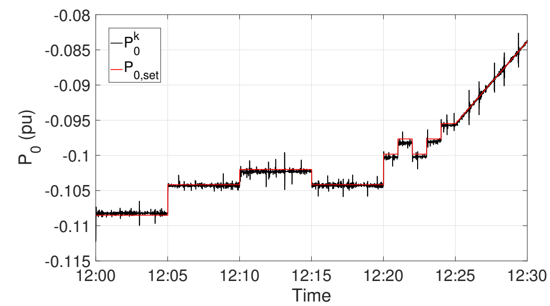

Fig. 1*: Real power at the feeder head for time period 12:00-12:30.*

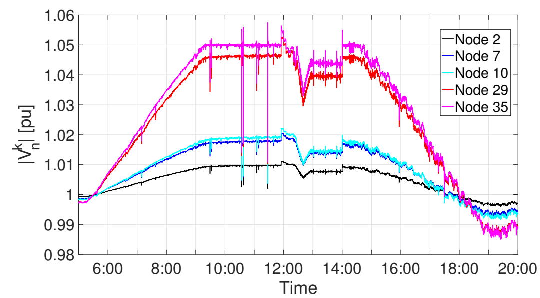

Fig. 2*: Voltage profile achieved (only some nodes are considered).*

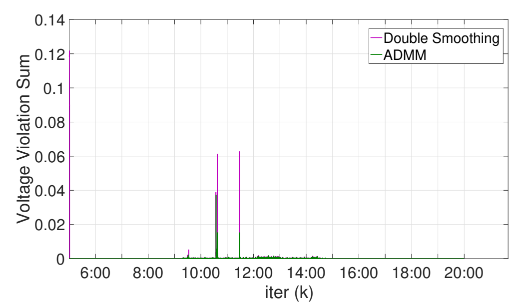

Fig. 3*: Index for the overall voltage violation across the system* $\sum_n \left(\max(|V_n^k| - V^{max}, 0) + \max(V^{min} - |V_n^k|, 0)\right)$

6. CONCLUSIONS AND FUTURE WORK

This paper proposed a feedback-based dynamic algorithm to optimize the performance of a distribution system in real time and systematically enforce operational constraints. For the synthesis of the algorithm, the steps of the ADMM were suitably modified to accommodate appropriate measurements from the distribution network and the DERs. With the aid of these measurements, the resultant algorithm can enforce operational constraints in spite of inaccuracies in the representation of the AC power flows. Future research efforts will focus on the application of similar techniques to time-varying nonconvex OPF problems.

This report is available at no cost from the National Renewable Energy Laboratory (NREL) at www.nrel.gov/publications.

7. REFERENCES

[1] J. A. Taylor, S. V. Dhople, and D. S. Callaway, "Power systems without fuel," *Renewable & Sustainable Energy Reviews*, 2015.

[2] S. Paudyaly, C. A. Canizares, and K. Bhattacharya, "Three-phase distribution OPF in smart grids: Optimality versus computational burden," in *2nd IEEE PES Intl. Conf. and Exhibition on Innovative Smart Grid Technologies*, Manchester, UK, Dec. 2011.

[3] A. Jokić, M. Lazar, and P. Van den Bosch, "Real-time control of power systems using nodal prices," *Intl. J. of Electrical Power & Energy Systems*, vol. 31, no. 9, pp. 522–530, 2009.

[4] J. Wang and N. Elia, "A control perspective for centralized and distributed convex optimization," in *Proc. of 50th IEEE Conf. on Decision and Control*, Orlando, FL, Dec. 2011.

[5] E. Dall'Anese, S. V. Dhople, and G. B. Giannakis, "Photovoltaic inverter controller seeking ac optimal power flow solutions," *IEEE Trans. Power Syst.*, 2015, to appear. [Online] Available at: http://arxiv.org/abs/1501.00188.

[6] L. Gan and S. H. Low, "An online gradient algorithm for optimal power flow on radial networks," *IEEE J. on Selected Areas in Commun.*, vol. 34, no. 3, pp. 625–638, Mar. 2016.

[7] A. Bernstein, L. Reyes Chamorro, J.-Y. Le Boudec, and M. Paolone, "A composable method for real-time control of active distribution networks with explicit power set points. part I: Framework," *Electric Power Systems Research*, vol. 125, no. Aug., pp. 254–264, 2015.

[8] Y. Zhang, M. Hong, E. Dall'Anese, S. V. Dhople, and Z. Xu, "Distributed controllers seeking ac optimal power flow solutions using admm," *IEEE Trans. Smart Grid*, Feb. 2017.

[9] S. Boyd, N. Parikh, E. Chu, B. Peleato, and J. Eckstein, "Distributed optimization and statistical learning via the alternating direction method of multipliers," *Foundations and Trends® in Machine Learning*, vol. 3, no. 1, pp. 1–122, 2011.

[10] T. Erseghe, "Distributed optimal power flow using ADMM," *IEEE Trans. Power Syst.*, vol. 29, no. 5, pp. 2370–2380, Sep. 2014.

[11] A. Hauswirth, S. Bolognani, G. Hug, and F. Dörfler, "Projected gradient descent on riemannian manifolds with applications to online power system optimization," in *Proc. of 54th Annual Allerton Conf. on Communication, Control, and Computing*, Sep. 2016.

[12] A. Hauswirth, A. Zanardi, S. Bolognani, G. Hug, and F. Dorfler, "Online optimization in closed loop on the power flow manifold," in *12th IEEE PES PowerTech conference*, 2017.

[13] Y. Tang, K. Dvijotham, and S. Low, "Real-time optimal power flow," *IEEE Trans. on Smart Grid*, 2017.

[14] A. Simonetto and G. Leus, "Double smoothing for time-varying distributed multiuser optimization," in *IEEE Global Conf. on Signal and Information Processing*, Dec. 2014, pp. 852–856.

[15] E. Dall'Anese and A. Simonetto, "Optimal power flow pursuit," *IEEE Trans. Smart Grid*, May 2016.

[16] H. He, S. Borhan, P. Kameshwar, and V. Tyrone L, "Aggregate flexibility of thermostatically controlled loads," *IEEE Trans. Power Syst.*, vol. 30, no. 1, pp. 189–198, Jan. 2015.

[17] S. Meyn, P. Barooah, A. Bušić, Y. Chen, and J. Ehren, "Ancillary service to the grid using intelligent deferrable loads," *IEEE Trans. Auto. Contr.*, vol. 60, no. 11, pp. 2847–2862, Nov. 2015.

[18] A. Baringo and L. Baringo, "A stochastic adaptive robust optimization approach for the offering strategy of a virtual power plant," *IEEE Trans. Power Syst.*, Dec. 2016.

[19] W. Kersting, "Distribution system modeling and analysis," in *Electric Power Generation, Transmission, and Distribution, Third Edition*, pp. 1–58. CRC press, 2012.

[20] S.V. Dhople, S. Guggilam, and Y. Chen, "Linear approximations to ac power flow in rectangular coordinates," in *Proc. of 53rd Annual Allerton Conf. on Communication, Control, and Computing*, Sep. 2015, pp. 211–217.

[21] S. Bolognani and F. Dörfler, "Fast power system analysis via implicit linearization of the power flow manifold," *Proc. of 53rd Allerton Conf. on Communication, Control, and Computing*, Sep. 2015.

[22] A. Bernstein and E. Dall'Anese, "Linear power-flow models in multiphase distribution networks," in *The 7th IEEE Intl. Conf. on Innovative Smart Grid Technologies*, Sep. 2017.

[23] J. Bank and J. Hambrick, "Development of a high resolution, real time, distribution-level metering system and associated visualization, modeling, and data analysis functions," Tech. Rep., National Renewable Energy Laboratory (NREL), Golden, CO., 2013.

This report is available at no cost from the National Renewable Energy Laboratory (NREL) at www.nrel.gov/publications.